Experimental Eye Research 271 (2026) 111170

Contents lists available at ScienceDirect

Experimental Eye Research

journal homepage: www.elsevier.com/locate/yexer

Research article

SPG302 mitigates diabetic retinal neuropathy and inner retinal damage in a genetic mouse model of diabetes

Peter W. Vanderklish [a,*], Tonking Bastola [b], Patrick Secrest [c], Maiah Brush [c], Muna Poudel [b], Ziyao Shen [b], Chung-Jui Yu [c], Savannah Pflugmacher [c], Stephanie Leal [c], Alex S. Huang [b], Srinivas R. Sadda [d,e], Robert N. Weinreb [b], Philip L.S.M. Gordts [c,f,g], Won-Kyu Ju [b,**], Christopher B. Toomey [c], Stella T. Sarraf [a]

[a] Spinogenix Inc., 1801 Century Park East, Suite 2400, Los Angeles, CA, USA
[b] Viterbi Family Department of Ophthalmology and Shiley Eye Institute, Hamilton Glaucoma Center, University of California San Diego, La Jolla, CA, USA
[c] Glycobiology Research and Training Center, Department of Medicine, University of California San Diego, La Jolla, CA, USA
[d] Doheny Eye Institute, Pasadena, CA, USA
[e] David Geffen School of Medicine, Department of Ophthalmology, University of California Los Angeles, Westwood, CA, USA
[f] University of Utah Molecular Medicine Program, University of Utah, Salt Lake City, UT, USA
[g] Department of Pathology, Division of Microbiology & Immunology, University of Utah School of Medicine, Salt Lake City, UT, USA

ARTICLE INFO

Keywords:
Diabetes
Retinal diabetic neuropathy
Ganglion cells
Synapses
SPG302
Tazbentetol
Visual function
Synaptic regeneration
Neuroprotection
Blindness
Glaucoma

ABSTRACT

Diabetic retinopathy (DR) is a leading cause of vision loss stemming from vascular and neurodegenerative sequelae of impaired glucose metabolism. Diabetic retinal neuropathy (DRN), an early feature of DR that can precede the microvasculopathy, is characterized by inner retinal degeneration with loss of ganglion cells (GCs) and impaired GC function, decreased inner retina synaptic markers, and increased reactive gliosis and cell death. Loss of glutamatergic synapses in the retina precedes, and may contribute to, overt neuron loss in DR, thus offering a potential new point for therapeutic intervention. SPG302, a novel pegylated benzothiazole derivative, promotes glutamatergic synaptogenesis and protects the inner retina in a mouse model of glaucoma, another leading cause of blindness associated with early synapse loss in the retina. To evaluate potential protective effects of SPG302 in DR, db/db mice (a diabetic mouse model with an inactivation mutation in the leptin receptor) were treated with intraperitoneal SPG302 or vehicle for 8 weeks (16-24 weeks of age). Db/+ mice served as an additional control. Db/db mice demonstrated weight gain, hyperglycemia, insulin intolerance, and glucose intolerance, while db/+ mice did not. SPG302 treatment did not change these metabolic parameters. Following treatment, GC function was assessed using electroretinography (ERG). Mice were then euthanized for quantification of retinal GCs, synaptic markers, glial markers, and markers of cell death using immunofluorescence staining and Western blot methods. Db/db mice demonstrated significant loss of GC ERG signal and GC cell number, decreased PSD95 and synaptophysin expression indicative of synapse loss, as well as increased reactive gliosis and expression of cell death markers such as pBAD and BAX. SPG302 treatment effectively preserved retinal integrity by reversing these changes. Thus, SPG302 has therapeutic potential for protecting the inner retina and mitigating DRN in diabetes.

1. Introduction

Diabetic retinopathy (DR) is a major cause of vision loss worldwide, and it has been estimated that DR will impact over 600 million people by 2040 (Ogurtsova, da Rocha Fernandes et al., 2017). DR presents in the eye with multiple findings, including retinal hemorrhages, macular edema, and proliferative changes (Kour et al., 2024). DR results from uncontrolled diabetes mellitus (DM) and high blood sugar, leading to microvascular degeneration and subsequent retinal damage (Durham and Herman, 2011). However, diabetic retinal neuropathy (DRN)

* Corresponding author.
** Corresponding author.
E-mail addresses: peter@spinogenix.com (P.W. Vanderklish), wju@health.ucsd.edu (W.-K. Ju).

https://doi.org/10.1016/j.exer.2026.111170
Received 16 May 2026; Received in revised form 24 June 2026; Accepted 14 July 2026
Available online 15 July 2026

stands apart as a retinal degeneration with axonal loss that has been reported to occur at the earliest stages of DR, commonly before vascular abnormalities are apparent (Sohn et al., 2016; Muc et al., 2018; Oshitari, 2021). Therefore, it has been proposed that a two-pronged therapeutic approach aimed at both the vascular and neurodegenerative features of DR may be more effective in mitigating the vision loss associated with diabetes.

Diabetic nerve damage is a well-accepted form of diabetic end-organ damage. This is most commonly described as peripheral neuropathy (causing neuropathic pain or numbness and tingling) or autonomic neuropathy (affecting the cardiovascular system and/or sex organs) (Muc et al., 2018; Strand et al., 2024). In the eye, DRN involves neuronal apoptosis and, in particular, affects the inner retina, with ganglion cell (GC) loss, reactive gliosis, inner-retina thinning, and corresponding deterioration of inner-retina functional tests, including visual field testing and electroretinography (ERG) (van Dijk et al., 2009; Sohn et al., 2016; Muc et al., 2018; Bao et al., 2019). In a longitudinal human study ($n = 45$) with an average follow-up of 5 years, OCT imaging in diabetics showed thinning of the perifoveal and parafoveal nerve fiber layer (NFL) and the GC plus inner plexiform layer (GCIPL), indicative of synapse loss, that was independent of A1c, sex, and age (Sohn et al., 2016). Results derived from post-mortem tissue from human donors with early DM demonstrated NFL thinning, without changes in the retinal capillary density (Sohn et al., 2016).

Along these lines, multiple DR animal models have shown DRN. Streptozotocin (STZ)-induced DM in mice resulted in time-dependent thinning of the inner retina by OCT and histology without evidence of changes to pericytes and capillaries (Sohn et al., 2016). The db/db mouse, which carries an inactivating mutation in the leptin receptor gene, is another useful model for studying diabetic retinal degeneration, as multiple groups have shown glial activation, increased apoptosis, progressive loss of GCs, reduced neuroretinal thickness, and diminished ERG responses (Bogdanov et al., 2014; Yang et al., 2015; Johnston et al., 2023). In all of these studies, the retinal degeneration was noted to occur at approximately 20-28 weeks of age.

Results from human and animal model studies indicate that synapse loss is among the earliest features of retinal pathology in diabetes (VanGuilder et al., 2008; Gaspar et al., 2010; Hombrebueno et al., 2014; Barber and Baccouche, 2017, McLaughlin et al., 2019; Albertos-Arranz et al., 2025). Notably, in STZ-induced DM rats, delayed insulin treatment and glycemic control were unable to reverse retinal synapse loss if already present, emphasizing the vulnerability of synaptic circuits and the need for early treatment to prevent their loss, or regenerative approaches to restore them (Masser et al., 2014). If inner retinal degeneration and axonal loss from DRN are one hallmark of early DR, then agents with synaptic or neuroprotective properties may offer a valuable additional therapeutic approach.

SPG302 is a new small molecule that targets the cytoskeleton and induces the formation of new glutamatergic synapses at low concentrations. In an Alzheimer's disease (AD) mouse model, daily dosing of SPG302 for 4 weeks increased the density of axospinous synapses – including both mushroom and stubby spine profiles – and the, expression of synaptic proteins (Trujillo-Estrada et al., 2021). In a rat spinal cord hemisection model for the effects of spinal cord injury on respiratory function, daily dosing of SPG302 for 2 weeks improved the recovery of diaphragm muscle function as assessed by electromyogram (Fogarty et al., 2023). In the eye, SPG302 demonstrated neuroprotective effects on the inner retina in a mouse model of glaucoma induced by microbead injection in the anterior chamber (Bastola et al., 2025). In these ocular hypertensive mice, SPG302 treatment preserved GCs, optic nerve axons, and retinal function as measured by patterned ERG (pERG) – specific to RGCs (Bastola et al., 2025). Extending from the above, SPG302 is now an orally bioavailable small molecule that is in clinical trials for AD, amyotrophic lateral sclerosis, and schizophrenia.

In view of these prior studies and the role of synapse loss in DRN pathogenesis, we hypothesized that SPG302 may confer similar benefits in DR. This manuscript describes the effects of daily systemic administration of SPG302 on GC loss and electrophysiological function, inner retina synaptic markers, glial activation, and markers of apoptosis in the db/db diabetic mouse model.

2. Materials and methods

2.1. Animals

The db/db (experimental) and db/+ (control) mice on a C57BL/6 background (The Jackson Laboratory, ME, USA) were acquired at 10 weeks of age and housed in covered cages, provided with a standard rodent diet ad libitum, and maintained on a 12-h light/dark cycle. Mice were weighed weekly and aged until 16 weeks at which point they were randomly assigned to receive SPG302 or control DMSO. The three arms of the study included (a) db/+ genetic controls treated with vehicle control (db/+ DMSO), (b) db/db mice treated with vehicle control (db/db DMSO), and (c) db/db treated with SPG302 (db/db SPG302). All animal research in this study adhered to the Association for Research in Vision and Ophthalmology (ARVO) Statement for the Use of Animals in Ophthalmic Vision Research and was performed under protocols approved by the Institutional Animal Care and Use Committee (IACUC) at the University of California, San Diego (CA, USA).

2.2. SPG302 administration

SPG302, provided by Spinogenix Inc., was stored at −80°C until use. SPG302 was administered by daily intraperitoneal (IP) injections at 30 mg/kg body weight, dissolved in PBS containing 2% DMSO. Control mice received daily IP injections of the vehicle solution (PBS containing 2% DMSO). Mice were injected daily from 16 weeks to 24 weeks of age, at which point they were sacrificed and tissues prepared for ocular studies.

2.3. Metabolic endpoint studies

Mice were fasted for 5-6 h prior to receiving the Insulin Tolerance Test (ITT) and Glucose Tolerance Test (GTT). Human insulin (0.35 U/kg; Sigma) in 0.9% NaCl/0.8% BSA in chow-fed mice and 2 g/kg sodium pyruvate in water were i.p. injected, and blood glucose levels from the tail vein were monitored after 15, 30, 60, 90, and 120 min. Two g/kg D-glucose in water was gavaged, and blood glucose levels were monitored after 20, 40, 60, and 90 min. Blood for insulin measurements was taken prior to and 20 min after glucose gavage via facial vein bleeding.

2.4. Tissue preparation

Mice were anesthetized via IP injection of a ketamine (100 mg/kg, Ketaset; Fort Dodge Animal Health, IA, USA) and xylazine (9 mg/kg, TranquiVed; Vedeco, Inc., MO, USA) mixture prior to cervical dislocation. For immunohistochemistry, retinas and optic nerve heads (ONHs) were carefully dissected from the choroids and fixed in 4% paraformaldehyde (Sigma-Aldrich) prepared in PBS (pH 7.4) for 2 h at 4°C. Following fixation, retinas and ONHs were washed multiple times with PBS, dehydrated through a graded ethanol series, and embedded in polyester wax.

2.5. Whole-mount immunohistochemistry and RGC counting

Retinas from enucleated eyes were dissected as flattened whole mounts. Retinas were immersed in PBS containing 30% sucrose for 24 h at 4°C. The retinas were blocked in PBS containing 3% donkey serum, 1% BSA, 1% fish gelatin, and 0.1% Triton X-100 and incubated with primary antibodies for 3 days at 4°C. The primary antibody used was a rabbit polyclonal anti-RBPMS antibody. After several wash steps, the retinas were incubated with Alexa Fluor-488 conjugated donkey anti-

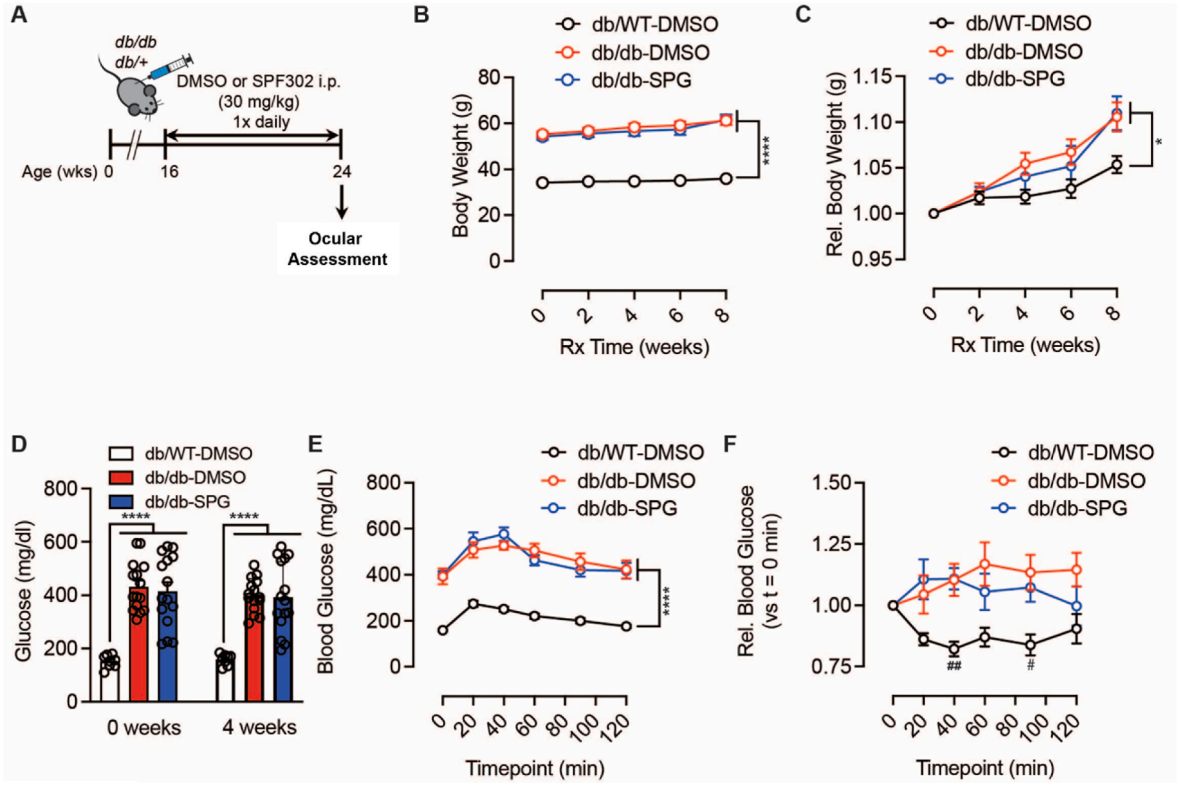

Fig. 1. Metabolic profile of db/+ DMSO mice, db/db DMSO mice, and db/db SPG302 mice. (A) Schematic of treatment regimen. (B-C) Absolute (B) and relative (C) weight gain during treatment ($n = 8$ to 15 mice per group). (D) Fasting blood glucose levels at 0 and 4 weeks of treatment ($n = 8$ to 15 mice per group). (E) Glucose tolerance test at 5 weeks of treatment ($n = 8$ to 15 mice per group). (F) Insulin tolerance test at 6 weeks of treatment ($n = 6$ to 15 mice per group). Error bars represent SEM. Statistical analysis was performed using one-way ANOVA and Tukey's multiple comparisons test. $^{*}P < 0.05$, $^{**}P < 0.01$, and $^{****}P < 0.0001$. $^{\#}P < 0.05$ and $^{\#\#}P < 0.01$ vs. T0 min.

rabbit IgG antibody or Alexa Fluor-568 conjugated donkey anti-mouse IgG antibody for 24 h and subsequently washed with PBS. Images were acquired using a Keyence All-in-One Fluorescence microscopy (BZ-X810, Keyence Corp. of America). RNA-binding protein with multiple splicing (RBPMS)- or Neuron-specific class III beta-tubulin (TUJ1)-positive RGCs were counted in the central, middle, and peripheral retina. The scores were averaged using ImageJ software [National Institutes of Health (NIH), MD, USA].

2.6. Immunohistochemistry

Immunohistochemical staining was performed on 7-μm wax sections of full-thickness retina and glial lamina. Sections from wax blocks ($n = 3$ mice per group) were used for analysis. To minimize nonspecific background staining, tissues were incubated in 1% bovine serum albumin (BSA, Sigma-Aldrich) in PBS for 1 h at room temperature, followed by incubation with primary antibodies for 16 h at 4°C. Primary antibodies used were a mouse monoclonal anti-TUJ1 antibody, a mouse monoclonal anti-glial fibrillary acidic protein (GFAP) antibody, and a rabbit polyclonal anti-Bax antibody. After several washes with PBS, tissue sections were incubated with the secondary antibodies, Alexa Fluor-488 conjugated donkey anti-rabbit IgG antibody or Alexa Fluor-568 conjugated donkey anti-mouse IgG antibody, for 4 h at 4°C and washed again. The sections were counterstained with Hoechst 33342 (1 μg/ml; Invitrogen, CA, USA) in PBS. Images were captured using a Keyence All-in-One Fluorescence Microscopy. The integrated fluorescence intensity of each target protein, expressed as pixels per area, was quantified using ImageJ (NIH), with imaging parameters held constant and background subtraction applied. The primary and secondary antibodies that were used are detailed in Supplementary Table S1.

2.7. Pattern electroretinogram (pERG) and pattern visual evoked potential (pVEP) analysis

pERG and pVEP were measured using the Celeris apparatus (Diagnosys, MA, USA), as described previously (Choi et al., 2020; Ju et al., 2023). After overnight dark adaptation, mice were anesthetized under red light using an intraperitoneal injection of a ketamine/xylazine cocktail. To dilate the pupils, a 0.5% tropicamide-2.5% phenylephrine mixture was applied to the eyes. Additionally, 1% proparacaine drops and 0.3% hypromellose gel were used to prevent corneal drying and cataract formation. pERG responses were recorded using alternating black-and-white vertical stimuli reversing at 1 Hz (2 reversals per second) with a luminance of 50 cd/m^2, delivered via a pattern stimulator. For each eye, 200 traces were recorded, and averaged waveforms were quantified by measuring amplitudes (μV) from the P1 peak to the N2 trough. Simultaneously, pVEP responses were captured. For pVEP recordings, a ground electrode was positioned subcutaneously at the tail, a reference electrode at the snout, and an active electrode subdermally at the midline of the head over the visual cortex. Each eye received 100 flashes of 1 Hz, 0.05 cd s/m^2 white light through corneal stimulators, with responses recorded over 300 ms at a sampling frequency of 2000 Hz. A total of 200 traces per eye were recorded, and averaged waveforms were quantified by measuring amplitudes (μV) from the P1 peak to the N1 trough. For each mouse, five trials were performed, with 100 sweeps per trial. The filter cutoffs for pVEP recordings were set to 1.25 Hz (low) and 100 Hz (high). All recordings were conducted while maintaining the body temperature between 37°C and 38°C using system heating pads. Data analysis was performed using Espion V6 software (Diagnosys) (Queirós et al., 2020; Gramlich et al., 2021).

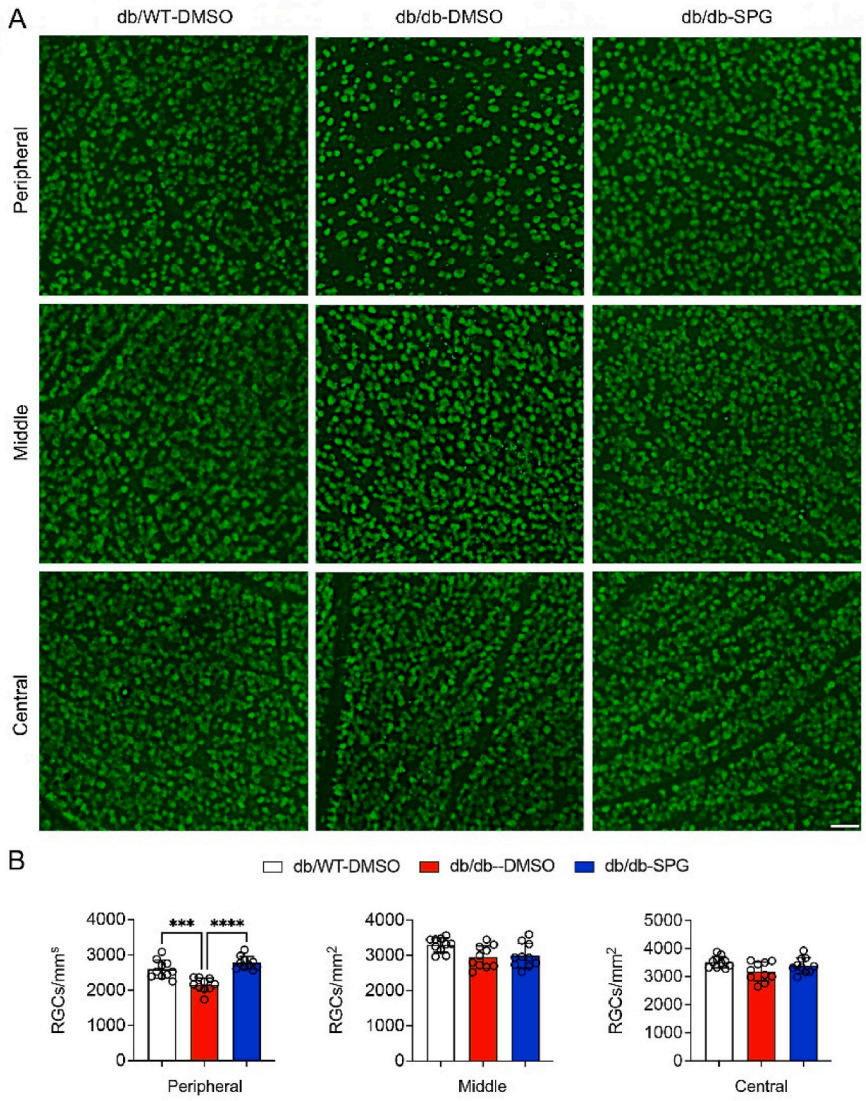

Fig. 2. SPG302 administration promotes RGC survival in db/db mice. (A) Representative retina wholemount images for RBPMS (green)-positive RGCs in the central, middle, and peripheral retina. (B) Quantitative analysis of RGC numbers in the peripheral, middle, and central areas of the retina ($n = 8$ to 10 mice per group). Error bars represent SEM. Statistical analysis was performed using one-way ANOVA and Tukey's multiple comparisons test. *$P < 0.05$, **$P < 0.01$, and ****P < 0.0001. Scale bars, 50 μm. (For interpretation of the references to colour in this figure legend, the reader is referred to the Web version of this article.)

2.8. Western blot

The collected retinas were homogenized for 1 min on ice using a RIPA lysis buffer [25 mM Tris-HCl, pH 7.6, 150 mM NaCl, 1% NP-40, 0.5% deoxycholic acid, 0.1% sodium dodecyl sulfate (SDS)] (Thermo Scientific), supplemented with a protease inhibitor cocktail (Thermo Scientific). Lysates were then centrifuged at 13,000 rpm for 15 min, and the protein concentration in the supernatants was measured using the BCA Protein Assay (Thermo Scientific). Proteins (10-15 μg) were loaded onto a 4-20% Mini-PROTEAN TGX-precast protein gel electrophoresis (Bio-Rad) and transferred to polyvinylidene difluoride (PVDF) membranes (Millipore Sigma). The membranes were blocked with TBS/0.1% Tween-20 (T-TBS) containing 5% skim milk for 1 h at room temperature and incubated with primary antibodies overnight at 4°C. Primary antibodies used were a mouse monoclonal anti-GFAP antibody, a rabbit polyclonal anti-Bax antibody, a rabbit polyclonal anti-Bcl-xL antibody, and a rabbit polyclonal anti-phospho-Bad (pBad) antibody. Membranes were washed three times with T-TBS and then incubated with horseradish peroxidase (HRP)-conjugated secondary antibodies (Cell Signaling Technology) for 1 h at room temperature. Signal was developed using an enhanced chemiluminescence (ECL) detection reagent (Bio-rad). The protein expression bands were visualized and captured using a ChemiDoc™ Imaging System (Bio-rad). The list of primary and secondary antibodies is provided in Supplementary Table S1.

2.9. Myelin staining

Myelin staining was examined on 5 μm wax sections of the optic nerve from each group. ON sections were incubated in 1% BSA/PBS for 1 h at room temperature to prevent non-specific background, then incubated with FluoroMyelin Red fluorescent myelin stain (Invitrogen, Carlsbad) for 1 h at RT. The tissues were then washed with PBS. Images were acquired using a Keyence All-in-One Fluorescence microscope, and the fluorescent intensity of FluoroMyelin in pixels per area was measured using the ImageJ software (National Institutes of Health). All imaging parameters were kept constant, and background subtraction was applied.

Table 1
Effect of SPG302 administration on RBPMS-positive RGC survival in the peripheral, middle, and central retina in db/db mice, related to Fig. 2.

Group	Sample size	RGC density per retina (RGCs/mm^2)		
		Peripheral	Middle	Central
Db/WT-DMSO	8	2595 ± 85	3292 ± 68	3516 ± 66
Db/db-DMSO	10	2151 ± 63	2949 ± 105	3175 ± 111
Db/db-SPG302	10	2776 ± 59	2989 ± 114	3392 ± 92

All results were reported as means ± SEM.

2.10. Statistical analysis

Data are shown as the mean standard error of the mean (SEM). Depending on the experimental design, a statistical multiple-group comparison or one-way ANOVA was applied. All statistical analyses were conducted using GraphPad Prism (GraphPad, CA, USA), with significance defined as $P < 0.05$.

3. Results

3.1. Metabolic profile of mice treated with or without SPG302

To evaluate the impact of SPG302 on obesity-associated DR, we aged homozygous leptin receptor-deficient mice (db/db) and control heterozygous mice on a normal chow diet. At 16 weeks old, mice were treated daily with either SPG302 (30 mg/kg body weight) or vehicle control (DMSO) for eight weeks and fed a normal chow diet (Fig. 1A). Db/db mice demonstrated increased weight gain, increased relative weight gain, higher fasting blood sugar, and impaired glucose and insulin tolerance compared to db/db mice (Fig. 1B–F). SPG302 treatment in db/db mice did not alter these parameters compared to db/db mice (Fig. 1B–F). These results indicate that SPG302 treatment did not affect weight gain or the extent of diabetes in db/db mice, which are the principle risk factors for the DR in this model system.

3.2. SPG302 administration protects RGCs in db/db mice

We evaluated the neuroprotective effects of the synaptic regenerative small molecule SPG302 on retinal ganglion cell (GC) survival in db/db mice. Quantitative GC analysis revealed a significant reduction in RGC density in the peripheral retina of db/db mice treated with DMSO compared with db/WT-DMSO controls, whereas no significant differences were observed in the middle or central retinal regions (Fig. 2A and B; Table 1). Notably, SPG302 treatment significantly improved GC survival in the peripheral retina of db/db mice, with no detectable effect in the middle or central regions (Fig. 2A and B; Table 1).

3.3. SPG302 administration ameliorates visual dysfunction in db/db mice

To evaluate the effects of SPG302 on visual function in db/db mice, we assessed pattern electroretinogram (pERG) and pattern visual evoked potential (pVEP) responses. Db/db-DMSO mice exhibited a significant reduction in RGC function, as indicated by decreased pERG amplitude compared with db/WT-DMSO controls (Fig. 3A; Table 2). While no significant change was observed by pVEP amplitude, pVEP latency revealed a significant conduction delay, reflected by increased latency

Table 2
Effect of SPG302 administration on pERG amplitude, pVEP amplitude, and pVEP latency from db/db mice, related to Fig. 3.

Group	Sample size	Visual function tests (pERG and pVEP)
		pERG Amplitude
Db/WT-DMSO	8	31.29 ± 1.11
Db/db-DMSO	10	16.31 ± 1.03
Db/db-SPG302	10	20.73 ± 1.03
		pVEP Amplitude
Db/WT-DMSO	8	23.16 ± 0.94
Db/db-DMSO	10	21.17 ± 1.78
Db/db-SPG302	10	24.13 ± 1.41
		pVEP Latency
Db/WT-DMSO	8	129.7 ± 7.57
Db/db-DMSO	10	192.4 ± 13.34
Db/db-SPG302	10	151.5 ± 10.16

All results were reported as means ± SEM.

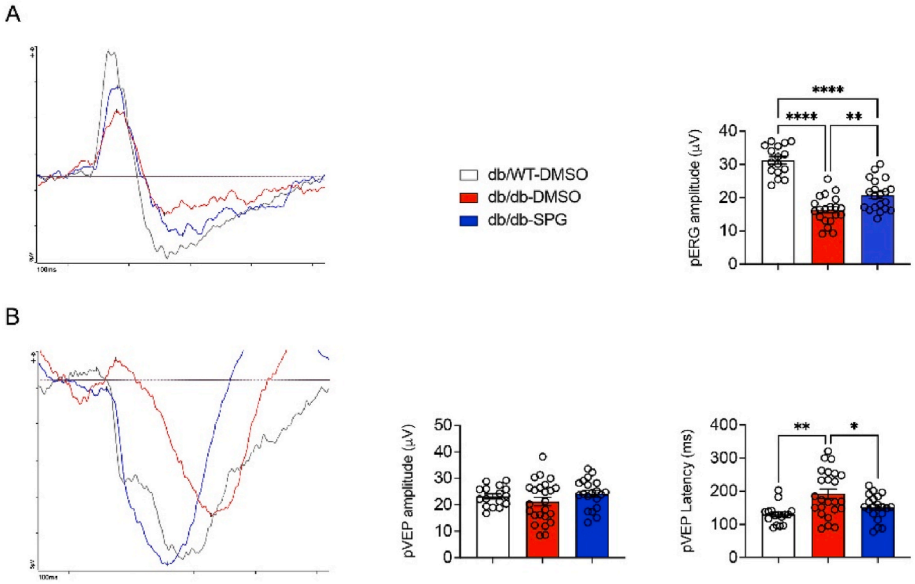

Fig. 3. SPG302 administration ameliorates visual dysfunction in db/db mice. (A) Representative recording graphs of pERG test. Quantitative analysis of pERG amplitude ($n = 8$ to 10 mice per group). (B) Representative recording graphs of pVEP test. Quantitative analysis of pVEP amplitude and latency ($n = 8$ to 10 mice per group). Error bars represent SEM. Statistical analysis was performed using one-way ANOVA and Tukey's multiple comparisons test. *$P < 0.05$, **$P < 0.01$ and ****$P < 0.0001$.

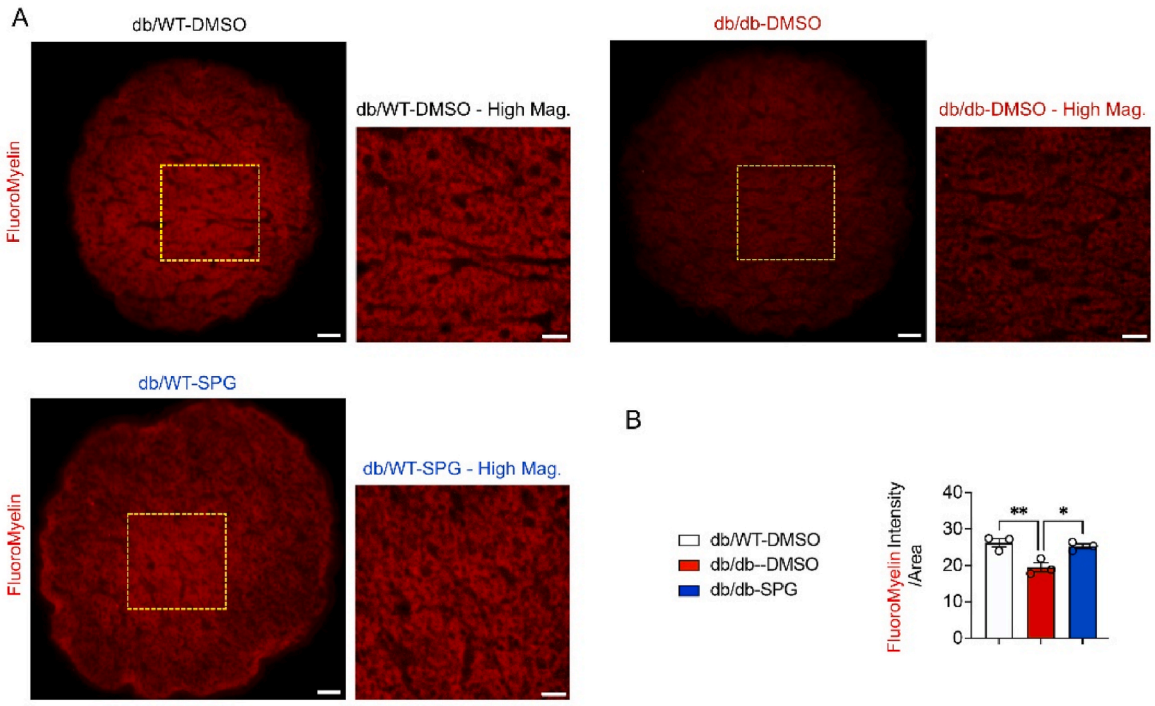

Fig. 4. SPG302 administration enhances FluoroMyelin Red intensity in the axons in the glial lamina of db/db mice. (A) Representative images from the glial lamina for FluoroMyelin Red (red)-positive axons. Note that higher magnification clearly shows a protective effect on myelin. (B) Quantitative analysis of FluoroMyelin Red intensity in the glial lamina ($n = 3$ mice per group). Error bars represent SEM. Statistical analysis was performed using one-way ANOVA and Tukey's multiple comparisons test. $^{*}P < 0.05$ and $^{**}P < 0.01$. Scale bars, 10 μm and 20 μm (high-mag.). (For interpretation of the references to colour in this figure legend, the reader is referred to the Web version of this article.)

(Fig. 3B; Table 2). Importantly, SPG302 treatment significantly improved RGC function and conduction in db/db mice, as evidenced by increased pERG amplitude and reduced pVEP conduction delay relative to db/db-DMSO mice (Fig. 3B; Table 2).

3.4. SPG302 administration preserves optic nerve myelination in db/db mice

Based on our observation that SPG302 mitigated pVEP conduction delay, we next examined whether SPG302 administration also preserves optic nerve myelination using FluoroMyelin Red fluorescent staining. FluoroMyelin Red intensity was significantly reduced in the glial lamina of db/db-DMSO mice compared with db/WT-DMSO controls (Fig. 4). Notably, SPG302 treatment significantly restored FluoroMyelin Red intensity in the glial lamina of db/db mice relative to db/db-DMSO mice (Fig. 4).

3.5. SPG302 administration preserved synapses in the retina of db/db mice

To evaluate the effect of SPG302 on synapses in the retina of db/db mice, we performed Western blot and immunohistochemical analyses of synaptophysin, a presynaptic marker, and PSD-95, a postsynaptic marker. Western blot analysis revealed no significant differences in synaptophysin or PSD-95 protein expression in retinal lysates from db/db-DMSO mice compared with controls (Fig. 5A). However, SPG302 treatment significantly increased PSD-95, but not synaptophysin, protein expression (Fig. 5A). In contrast, immunohistochemical analysis allows more specific focus on the inner plexiform layer (IPL), and synaptophysin and PSD-95 immunoreactivities were markedly reduced in the db/db-DMSO mice (Fig. 5B–E). SPG302 administration significantly increased synaptophysin and PSD-95 immunoreactivities in the IPL of db/db mice (Fig. 5D and E), suggesting preservation of retinal synaptic integrity.

3.6. SPG302 administration inhibits glial activation in the retina of db/db mice

To evaluate the effect of SPG302 on glial activation in the retina of the db/db model, we performed immunohistochemical analysis of GFAP. Db/db-DMSO mice exhibited a significant increase in GFAP protein expression in retinal lysates compared with controls (Fig. 6A). In contrast, SPG302 treatment significantly reduced GFAP expression, indicating inhibition of retinal astrocyte activation (Fig. 6A). Consistent with these findings, GFAP immunoreactivity was markedly increased in the ganglion cell layer (GCL) and inner plexiform layer (IPL) of db/db-DMSO mice (Fig. 6B and C), whereas SPG302 administration significantly attenuated GFAP immunoreactivity in both layers in db/db mice (Fig. 6B and C).

3.7. SPG302 administration inhibits apoptotic cell death in the retina of db/db mice

To evaluate the effect of SPG302 on apoptotic cell death in the retina of the db/db model, we performed immunohistochemical analysis of apoptotic cell death markers, Bcl-xL, Bax, and pBad. Db/db-DMSO mice exhibited a significant decrease in Bcl-xL protein expression in retinal lysates compared with controls, along with an increased expression pattern of Bax and pBad (Fig. 7A). In contrast, SPG302 treatment significantly increased Bcl-xL protein expression but decreased Bax and pBad protein expression, suggesting inhibition of apoptotic cell death signaling (Fig. 7A). Consistent with these findings, Bax immunoreactivity was markedly increased in the GCL of db/db-DMSO mice (Fig. 7B and C), whereas SPG302 administration significantly diminished immunoreactivity in the GCL of db/db mice (Fig. 7B and C).

4. Discussion

This work demonstrates that SPG302 can mitigate inner retinal

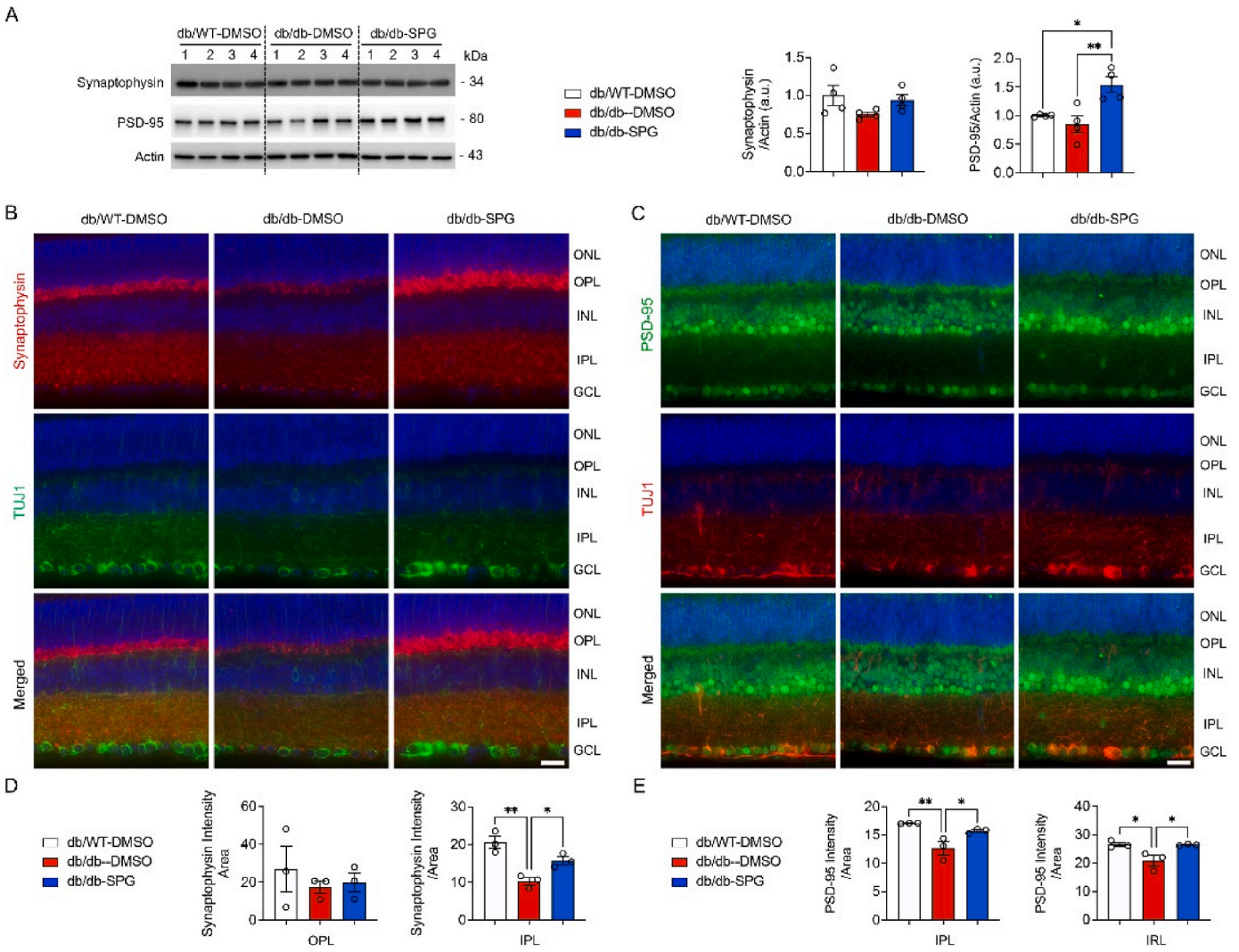

Fig. 5. SPG302 administration preserves synaptophysin and PSD-95 protein expression in db/db mice. (A) Quantitative analysis of synaptophysin and PSD-95 protein expression in the retina ($n = 3$ mice per group). (B and C) Representative retinal section images for synaptophysin (red), PSD-95 (green), and TUJ1 protein expression. (D and E) Quantitative analysis of synaptophysin and PSD-95 intensity in the OPL, IPL, or inner retinal layer (IRL) ($n = 3$ mice per group). Error bars represent SEM. Statistical analysis was performed using one-way ANOVA and Tukey's multiple comparisons test. $^{*}P < 0.05$ and $^{**}P < 0.01$. Scale bars, 20 μm. (For interpretation of the references to colour in this figure legend, the reader is referred to the Web version of this article.)

degeneration in a genetic mouse model of diabetes. As expected, the db/db mouse showed increased weight gain and blood sugar as well as impaired glucose and insulin tolerance (Fig. 1). Eyes in this model showed inner retinal damage with loss of GCs (Fig. 2), deficits in GC function as measured by pERG (Fig. 3), and reduced expression of synaptic markers (Fig. 5). There also was increased expression of gliotic (Fig. 6) and cell death markers (Fig. 7). Treatment with SPG302 preserved GCs (Fig. 2) and their neurophysiological function (Fig. 3). Furthermore, SPG302 promoted the expression of pre- and postsynaptic markers in the inner plexiform layer (Fig. 5), consistent with its known pro-synaptic effects. SPG302 also mitigated reactive gliosis (Fig. 6) as well as markers of apoptosis in the inner retina while improving a cell-survival marker (Fig. 7). These results are likely direct effects of SPG302 on the retina, as metabolic studies did not show that SPG302 changed db/db mouse weight, blood sugar levels, or glucose or insulin tolerance (Fig. 1). Based upon these results, SPG302 appears to be a promising neuroprotective therapy for DRN in DR.

The efficacy of SPG302 in a model of DR essentially mirrors our prior findings of neuroprotective effects in a glaucoma model (Bastola et al., 2025). Notably, DRN affects the same retinal regions and cells as OHTN in glaucoma. As in DR, inner plexiform synaptic loss is one of the earliest disease features in glaucoma, leading to loss of GCs, retinal nerve fiber layer, and ultimately visual field (Kostovic et al., 1989; Ou et al., 2016). In both studies, SPG302's effects were present at both a cellular/structural level and a functional electrophysiological level (Bastola et al., 2025). Thus, these two models serve as two independent stressors (OHTN and hyperglycemia from an inactivating mutation in the leptin receptor gene) where SPG302 shows reproducible inner retina neuroprotection.

While electrophysiological improvement in pERG amplitudes was a hypothesized effect of SPG302, the improvement in delayed VEP latency that we observed (Fig. 4) was unexpected. This same endpoint was tested in the glaucoma study (Bastola et al., 2025), and neither OHTN nor SPG302 altered VEP latency. For DR, delayed VEP latency has been observed in patients since the 1980s and reproduced in diabetic animal models (Yaltkaya et al., 1988; Ozkaya et al., 2007; Ghita et al., 2013; Miura, 2023). Regarding the cause, there is conflicting evidence on the relationship between delayed VEP latency and blood sugar levels (Miura, 2023). Despite this, DM has been associated with abnormal nerve myelination, as streptozotocin-induced diabetic mice have shown abnormal oligodendrocytes and decreased myelin deposition on the optic nerve (Wu et al., 2023). Myelination improves nerve conduction

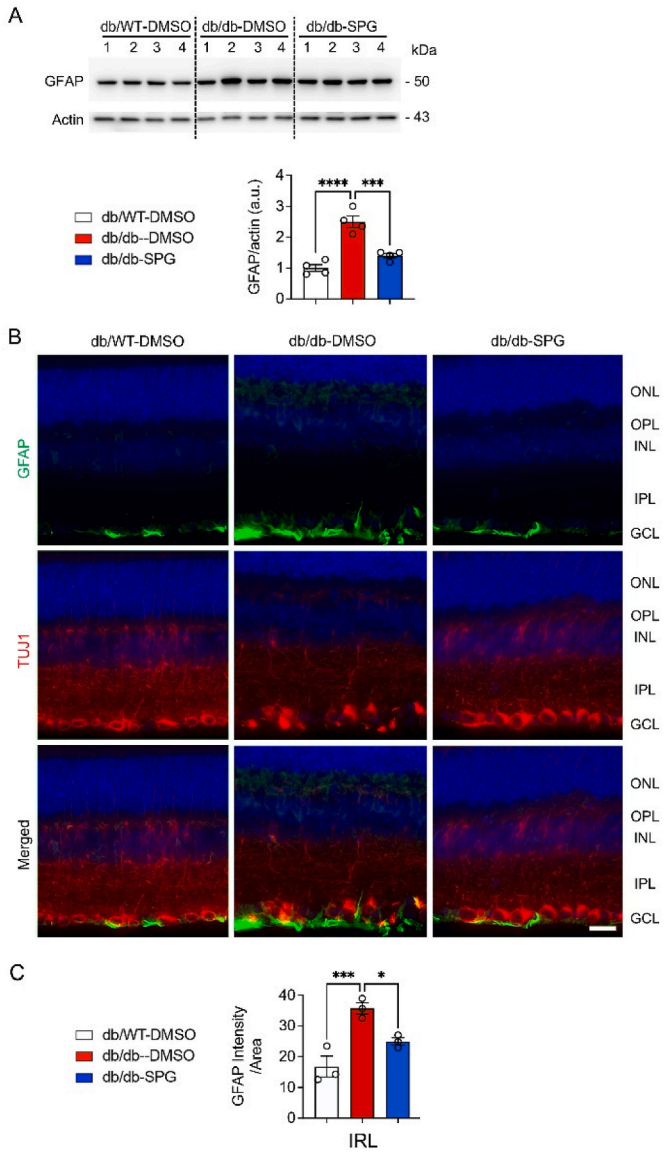

Fig. 6. SPG302 administration preserves GFAP protein expression in db/db mice. (A) Quantitative analysis of GFAP protein expression in the retina ($n = 3$ mice per group). (B) Representative retinal section images for GFAP (green) and TJU1 (red) protein expression. (C) Quantitative analysis of GFAP intensity in the inner retinal layer (IRL) ($n = 3$ mice per group). Error bars represent SEM. Statistical analysis was performed using one-way ANOVA and Tukey's multiple comparisons test. *$P < 0.05$, ***$P < 0.001$, and ****$P < 0.0001$. Scale bars, 20 μm. (For interpretation of the references to colour in this figure legend, the reader is referred to the Web version of this article.)

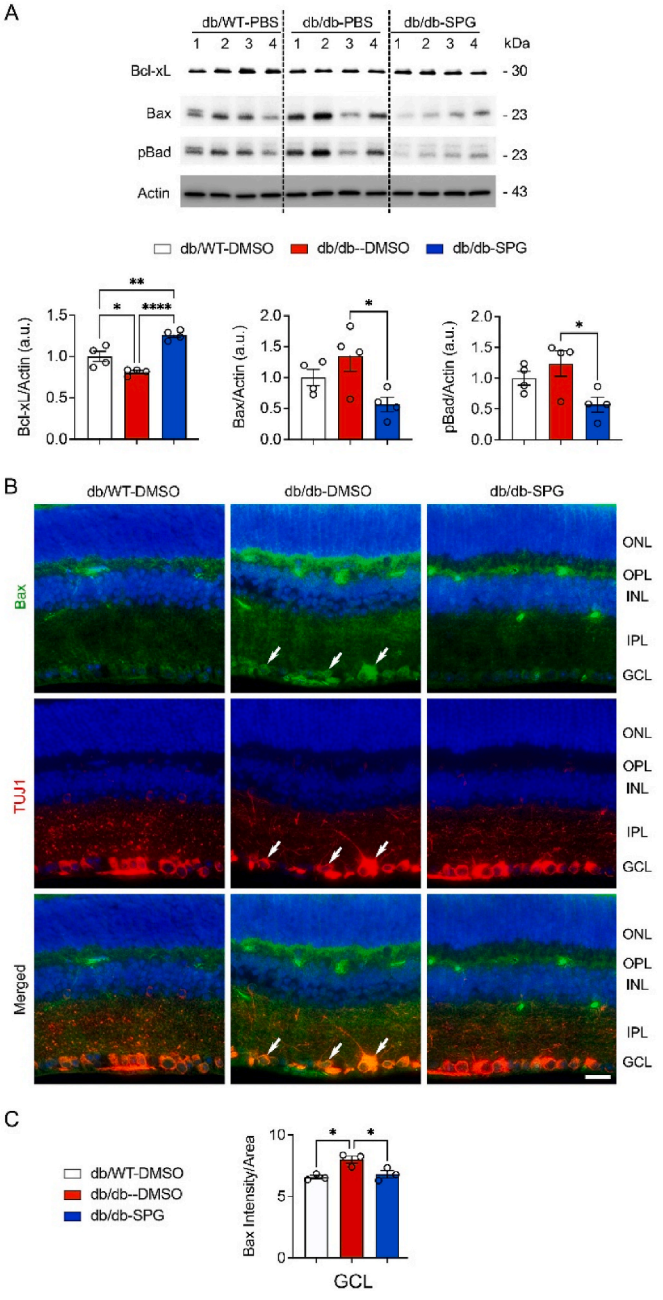

Fig. 7. SPG302 administration increases Bcl-xL protein expression but decreases Bax and pBad protein expression in db/db mice. (A) Quantitative analysis of Bcl-xL, Bax, and pBad protein expression in the retina ($n = 3$ mice per group). (B) Representative retinal section images for Bax (green) and TUJ1 (red) protein expression. Arrowheads indicate Bax-positive RGCs. (C) Quantitative analysis of Bax intensity in the GCL ($n = 3$ mice per group). Error bars represent SEM. Statistical analysis was performed using one-way ANOVA and Tukey's multiple comparisons test. *$P < 0.05$, **$P < 0.01$, and ****$P < 0.0001$. Scale bars, 20 μm. (For interpretation of the references to colour in this figure legend, the reader is referred to the Web version of this article.)

efficiency (Franssen, 2019), and delayed VEP latency is often associated with demyelinating diseases such as optic neuritis (Hely et al., 1986; Petzold et al., 2022). In our study, we also demonstrated diminished myelin staining in the db/db optic nerve – plausibly explaining the increased VEP latency – and this was improved after SPG302 administration (Fig. 4). Therefore, the relationship between SPG302 and myelination should be studied and better understood.

Overall, SPG302 is a new class of potent, rapid-acting, synaptic regenerative small molecule that has been shown to restore dendritic spine synapses and improve function in multiple model systems. At both a cellular and functional level, SPG302 has already been shown to improve synaptic function in the brain (in a triple transgenic AD model) (Trujillo-Estrada et al., 2021), spinal cord (in a spinal cord hemisection model) (Fogarty et al., 2023), and eye (in an ocular hypertension glaucoma model) (Bastola et al., 2025). Both in the glaucoma paper (Bastola et al., 2025) and this work, PSD95 is noted to be higher after SPG302 treatment than in the control. Thus, we add to the literature by showing improved inner retinal synaptic structure and function in a diabetic mouse model. Further work is warranted to study why this postsynaptic marker was greater than in the control (db/+) condition and if it represents reversal of some baseline level of synaptopathy attending partial reduction of leptin signaling in the mouse retina

(Shanley et al., 2001). These and other findings have prompted the initiation of clinical trials of SPG302 as a once-a-day orally bioavailable synaptic regenerative therapy (tazbentetol) in multiple indications that involve the loss of axospinous glutamatergic synapses: amyotrophic lateral sclerosis (NCT05882695), Alzheimer's disease (NCT06427668), and schizophrenia (NCT06442462). We propose that a similar strategy can be employed to treat DRN in DR.

This study has a number of limitations. Only a single dose of SPG302 (30 mg/kg) was evaluated, chosen based on prior animal research (Trujillo-Estrada et al., 2021; Fogarty et al., 2023) that demonstrated rescue of synaptic density and behavioral function. While SPG302 is readily brain-penetrant in internal studies, the efficiency of drug delivery to the inner retina may differ despite (a) similarities in the blood: retinal and blood:brain barriers (Toda et al., 2011) and (b) reports that the retinal blood vasculature may be leakier than the brain vasculature in diabetes (Li et al., 2021). Therefore, exploring additional doses would elucidate the dose dependence of SPG302's neuroprotective effects in DRN. This study also did not investigate the potential benefits of SPG302 on synaptic transmission deficits in the brain observed in diabetes (Zeng et al., 2026), which can accompany DRN and contribute to visual and cognitive/memory dysfunction (Yermakov et al., 2019). SPG302 has been shown to improve Morris water maze performance in an AD mouse model (Trujillo-Estrada et al., 2021). Therefore, future studies of SPG302's therapeutic benefits could include testing its effects on behavioral and neuroanatomical deficits associated with diabetes. Lastly, diabetes can impact peripheral nerves as well. However, the impact of SPG302 on peripheral nerves is not known and can be studied in the future.

In summary, SPG302 demonstrates therapeutic potential for inner retina protection and preservation of visual function in DRN. Further research is needed to elucidate the exact mechanisms by which SPG302 safeguards and maintains the structural and functional integrity of the inner retina. In the future, SPG302 can be explored as a neuroprotective agent to treat DR.

Informed consent statement

Not applicable.

Institutional review board statement

Not applicable.

Funding

This study was supported by National Institutes of Health grants EY031697, EY036155 and P30 EY022589 (Vision core grant), and a research grant from Spinogenix Inc.

CRediT authorship contribution statement

Peter W. Vanderklish: Conceptualization, Funding acquisition, Methodology, Supervision, Writing – original draft. **Tonking Bastola:** Data curation, Investigation, Writing – review & editing. **Patrick Secrest:** Data curation, Investigation, Writing – review & editing. **Maiah Brush:** Data curation, Investigation, Writing – review & editing. **Muna Poudel:** Data curation, Investigation, Writing – review & editing. **Ziyao Shen:** Data curation, Investigation, Writing – review & editing. **Chung-Jui Yu:** Data curation, Investigation, Writing – review & editing. **Savannah Pflugmacher:** Data curation, Investigation, Writing – review & editing. **Stephanie Leal:** Data curation, Investigation, Writing – review & editing. **Alex S. Huang:** Conceptualization, Formal analysis, Funding acquisition, Methodology, Supervision, Validation, Writing – original draft. **Srinivas R. Sadda:** Conceptualization, Methodology, Writing – review & editing. **Robert N. Weinreb:** Conceptualization, Methodology, Writing – review & editing. **Philip L.S.M. Gordts:** Conceptualization, Formal analysis, Funding acquisition, Methodology, Supervision, Validation, Writing – original draft. **Won-Kyu Ju:** Conceptualization, Formal analysis, Funding acquisition, Methodology, Supervision, Validation, Writing – original draft. **Christopher B. Toomey:** Conceptualization, Formal analysis, Funding acquisition, Methodology, Supervision, Validation, Writing – original draft. **Stella T. Sarraf:** Conceptualization, Funding acquisition, Methodology, Supervision, Writing – review & editing.

Conflicts of interest

PWV: Spinogenix (E); TB: none; PS: none; BM: none; MP: none; CJY: none; SP: none; SL: none; ASH: Amydis (C), Celanese (C), Diagnosys (F), Balance (C), Heidelberg Engineering (F), Iantrek (C), QLARIS (C), Santen (C), Spinogenix (C), and Topcon (C); SRS: Consultant: Allergan/Abbvie, Alexion, Amgen, CharacterBio, Eyetem, Apellis, Bayer, Regeneron, Roche/Genentech, Novartis, NGMBio, Neurotech, ONL Tx, Nanoscope, 4dMT, OcularTx, NotalVision, Astellas, Oxurion, Eyepoint, Boerhinger Ingelheim, Optos, Heidelberg Engineering, iCare, Topcon, Samsung Bioepis; Research Instruments: Intalight, Topcon, Nidek, Carl Zeiss Meditec, Optos, Heidelberg, iCare; RNW: RNW: Amydis (C), Spinogenix (C), Topcon (C); PLSMG: Gallant Bio (C); WKJ: none; CBT: Alnylam Pharmaceuticals (C); STS: Spinogenix (O).

Appendix A. Supplementary data

Supplementary data to this article can be found online at https://doi.org/10.1016/j.exer.2026.111170.

Data availability

Data will be made available on request.

References

Albertos-Arranz, H., et al., 2025. Neuronal degeneration and glial activation in the absence of vascular changes in human retinas of patients with diabetes. Investig. Ophthalmol. Vis. Sci. 66 (3), 53.
Bao, Y.K., et al., 2019. Visual field loss in patients with diabetes in the absence of clinically-detectable vascular retinopathy in a nationally representative survey. Investig. Ophthalmol. Vis. Sci. 60 (14), 4711–4716.
Barber, A.J., Baccouche, B., 2017. Neurodegeneration in diabetic retinopathy: potential for novel therapies. Vis. Res. 139, 82–92.
Bastola, T., et al., 2025. SPG302 protects retinal ganglion cells and preserves visual function by preserving synaptic activity in a mouse model of glaucoma. Exp. Eye Res. 261, 110640.
Bogdanov, P., et al., 2014. The db/db mouse: a useful model for the study of diabetic retinal neurodegeneration. PLoS One 9 (5), e97302.
Choi, S.H., et al., 2020. AIBP protects retinal ganglion cells against neuroinflammation and mitochondrial dysfunction in glaucomatous neurodegeneration. Redox Biol. 37, 101703.
Durham, J.T., Herman, I.M., 2011. Microvascular modifications in diabetic retinopathy. Curr. Diabetes Rep. 11 (4), 253–264.
Fogarty, M.J., et al., 2023. Novel regenerative drug, SPG302 promotes functional recovery of diaphragm muscle activity after cervical spinal cord injury. J. Physiol. 601 (12), 2513–2532.
Franssen, H., 2019. Physiology of myelinated nerve conduction and pathophysiology of demyelination. Adv. Exp. Med. Biol. 1190, 85–106.
Gaspar, J.M., et al., 2010. Diabetes differentially affects the content of exocytotic proteins in hippocampal and retinal nerve terminals. Neuroscience 169 (4), 1589–1600.
Ghita, A.M., et al., 2013. Electrophysiological changes in optic neuropathy of streptozotocin induced diabetic rats. J. Med. Life 6 (3), 340–348.
Gramlich, O.W., et al., 2021. Early functional impairment in experimental glaucoma is accompanied by disruption of the GABAergic system and inceptive neuroinflammation, 22 (14), 7581.
Hely, M.A., et al., 1986. Visual evoked responses and ophthalmological examination in optic neuritis. A follow-up study. J. Neurol. Sci. 75 (3), 275–283.
Hombrebueno, J.R., et al., 2014. Loss of synaptic connectivity, particularly in second order neurons is a key feature of diabetic retinal neuropathy in the Ins2Akita mouse. PLoS One 9 (5), e97970.
Johnston, T.P., et al., 2023. Synergism of mechanisms underlying early-stage changes in retina function in male hyperglycemic db/db mice in the absence and presence of chemically-induced dyslipidemia. Sci. Rep. 13 (1), 17347.

Ju, W.K., et al., 2023. Restoring AIBP Expression in the Retina Provides Neuroprotection in Glaucoma. bioRxiv.
Kostovic, I., et al., 1989. Structural basis of the developmental plasticity in the human cerebral cortex: the role of the transient subplate zone. Metab. Brain Dis. 4 (1), 17–23.
Kour, V., et al., 2024. A review on diabetic retinopathy. Curr. Diabetes Rev. 20 (6), e201023222418.
Li, Y., et al., 2021. Comparative transcriptome analysis of inner blood-retinal barrier and blood-brain barrier in rats. Sci. Rep. 11 (1), 12151.
Masser, D.R., et al., 2014. Insulin treatment normalizes retinal neuroinflammation but not markers of synapse loss in diabetic rats. Exp. Eye Res. 125, 95–106.
McLaughlin, T., et al., 2019. Loss of XBP1 leads to early-onset retinal neurodegeneration in a mouse model of type I diabetes. J. Clin. Med. 8 (6).
Miura, G., 2023. Visual evoked potentials for the detection of diabetic retinal neuropathy. Int. J. Mol. Sci. 24 (8).
Muc, R., et al., 2018. Associations of diabetic retinopathy with retinal neurodegeneration on the background of diabetes mellitus. Overview of recent medical studies with an assessment of the impact on healthcare systems. Open Med. 13, 130–136.
Ogurtsova, K., et al., 2017. IDF diabetes atlas: global estimates for the prevalence of diabetes for 2015 and 2040. Diabetes Res. Clin. Pract. 128, 40–50.
Oshitari, T., 2021. The pathogenesis and therapeutic approaches of diabetic neuropathy in the retina. Int. J. Mol. Sci. 22 (16).
Ou, Y., et al., 2016. Selective vulnerability of specific retinal ganglion cell types and synapses after transient ocular hypertension. J. Neurosci. 36 (35), 9240–9252.
Ozkaya, Y.G., et al., 2007. Exercise improves visual deficits tested by visual evoked potentials in streptozotocin-induced diabetic rats. Tohoku J. Exp. Med. 213 (4), 313–321.
Petzold, A., et al., 2022. Diagnosis and classification of optic neuritis. Lancet Neurol. 21 (12), 1120–1134.
Queirós, A., et al., 2020. Retinal response of low myopes during orthokeratology treatment, 9 (8), 2649.
Shanley, L.J., et al., 2001. Leptin enhances NMDA receptor function and modulates hippocampal synaptic plasticity. J. Neurosci. 21 (24).
Sohn, E.H., et al., 2016. Retinal neurodegeneration may precede microvascular changes characteristic of diabetic retinopathy in diabetes mellitus. Proc. Natl. Acad. Sci. U. S. A. 113 (19), E2655–E2664.
Strand, N., et al., 2024. Diabetic neuropathy: pathophysiology review. Curr. Pain Headache Rep. 28 (6), 481–487.
Toda, R., et al., 2011. Comparison of drug permeabilities across the blood-retinal barrier, blood-aqueous humor barrier, and blood-brain barrier. J. Pharmaceut. Sci. 100 (9), 3904–3911.
Trujillo-Estrada, L., et al., 2021. SPG302 reverses synaptic and cognitive deficits without altering amyloid or tau pathology in a transgenic model of Alzheimer's disease. Neurotherapeutics 18 (4), 2468–2483.
van Dijk, H.W., et al., 2009. Selective loss of inner retinal layer thickness in type 1 diabetic patients with minimal diabetic retinopathy. Investig. Ophthalmol. Vis. Sci. 50 (7), 3404–3409.
VanGuilder, H.D., et al., 2008. Diabetes downregulates presynaptic proteins and reduces basal synapsin I phosphorylation in rat retina. Eur. J. Neurosci. 28 (1), 1–11.
Wu, H., et al., 2023. Deficient deposition of new myelin impairs adult optic nerve function in a murine model of diabetes. Glia 71 (5), 1333–1345.
Yaltkaya, K., et al., 1988. Visual evoked potentials in diabetes mellitus. Acta Neurol. Scand. 77 (3), 239–241.
Yang, Q., et al., 2015. Retinal neurodegeneration in db/db mice at the early period of diabetes. J. Ophthalmol. 2015, 757412.
Yermakov, L.M., et al., 2019. Impairment of cognitive flexibility in type 2 diabetic db/db mice. Behav. Brain Res. 371, 111978.
Zeng, Y., et al., 2026. Early diabetes impairs visual function in mice through altering neuronal activity in the primary visual cortex. IBRO Neurosci. Rep. 20, 5–13.